PHAGOCYTOSIS OF BACTERIA BY POLYMORPHONUCLEAR LEUKOCYTES

A Freeze-Fracture, Scanning Electron Microscope, and Thin-Section Investigation of Membrane Structure

P. L. MOORE, H. L. BANK, N. T. BRISSIE, and S. S. SPICER

From the Pathology Department, Medical University of South Carolina, Charleston, South Carolina 29401. Dr. Moore's present address is the Biology Department, Yale University, New Haven, Connecticut 06520.

ABSTRACT

The changes in membrane structure of rabbit polymorphonuclear (PMN) leukocytes during bacterial phagocytosis was investigated with scanning electron microscope (SEM), thin-section, and freeze-fracture techniques. SEM observations of bacterial attachment sites showed the involvement of limited areas of PMN membrane surface (0.01–0.25 μm^2). Frequently, these areas of attachment were located on membrane extensions. The membrane extensions were present before, during, and after the engulfment of bacteria, but were diminished in size after bacterial engulfment. In general, the results obtained with SEM and thin-section techniques aided in the interpretation of the three-dimensional freeze-fracture replicas. Freeze-fracture results revealed that PMN leukocytes had two fracture faces as determined by the relative density of intramembranous particles (IMP). Membranous extensions of the plasma membrane, lysosomes, and phagocytic vacuoles contained IMPs with a distribution and density similar to those of the plasma membrane.

During phagocytosis, IMPs within the plasma membrane did not undergo a massive aggregation. In fact, structural changes within the membranes were infrequent and localized to regions such as the attachment sites of bacteria, the fusion sites on the plasma membrane, and small scale changes in the phagocytic vacuole membrane during membrane fusion. During the formation of the phagocytic vacuole, the IMPs of the plasma membrane appeared to move in with the lipid bilayer while maintaining a distribution and density of IMPs similar to those of the plasma membranes. Occasionally, IMPs were aligned in linear arrays within phagocytic vacuole membranes. This alignment might be due to an interaction with linearly arranged motile structures on the side of phagocytic vacuole membranes. IMP-free regions were observed after fusion of lysosomes with the phagocytic vacuoles or plasma membrane. These IMP-free areas probably represent sites where membrane fusion occurred between lysosomal membrane and phago-

cytic vacuole membrane or plasma membrane. Highly symmetrical patterns of IMPs were not observed during lysosomal membrane fusion.

KEY WORDS phagocytosis · membrane structure · leukocytes · bacteria · microfilaments and microtubules · lysosomes

The importance of phagocytosis by neutrophilic leukocytes in inflammation is well established (25, 36, 72). During inflammation one of the primary functions of polymorphonuclear (PMN) leukocytes is to phagocytize bacteria. This process of phagocytosis involves a number of endocytic and exocytic membrane events each of which appears to be a prerequisite for the destruction of the invading bacteria. These membrane events include (*a*) the attachment of opsonized (serum-coated) bacteria to the leukocytes (60), (*b*) the engulfment of the bacteria, (*c*) the formation of phagocytic vacuoles (24, 27, 33, 75), (*d*) the fusion of lysosomal and phagocytic vacuole membranes (24, 27, 33, 75), and (*e*) the concomitant secretion of lysosomal enzymes into the phagocytic vacuole and extracellular medium (73). Since phagocytosis has so many naturally occurring membrane events, it is an excellent model system for the study of membrane structure and interactions.

Previous ultrastructural studies of phagocytosis provide useful information on the chronology of membrane events (24, 27, 33, 75), and on the size, shape, and cross-sectional thickness of membranes (33, 69, 75). However, these studies provide little information about the external and internal structure of membranes during phagocytosis. Information about the external features of membrane surfaces can now be obtained with scanning electron microscope techniques while information about the internal structure of membranes can be obtained with freeze-fracture techniques.

Freeze-fractured membranes tend to fracture along their inner hydrophobic region (45), revealing the presence of intramembranous particles on both of the exposed fracture faces of the membrane. These intramembranous particles are believed to be composed, at least in part, of glycoproteins (64) and appear to be asymmetrically distributed across the lipid bilayer (67, 68). It is also known that a variety of agents including multivalent ligands (46, 64), viruses (64), certain conditions of pH, divalent ion concentration (44, 14), and enzyme treatments (16) aggregates intramembranous particles. These observations have led several authors (see Steck's review, reference 58) to suggest that intramembranous particles might be linked either directly or indirectly to peripheral membrane proteins. Since there is evidence that actin filaments may be attached either directly or indirectly to membranes (26, 48, 49, 54, 65, 66), it is thought that contractile proteins interact with intramembranous particles.

Satir et al. (52) have reported another type of aggregation of intramembranous particles which occurs during membrane fusion during *Tetrahymena* mucocyst secretion. These aggregated IMPs form rosettes and are thought to be inducible membrane sites which precede and perhaps trigger membrane fusion. Although rosettes are indisputably present during protozoan membrane fusion, it is not certain that these structures are present in mammalian membrane fusion. Recent research on mast cell secretion (10, 11, 31) and on ionophore A23187-induced lysosomal release in PMN leukocytes (40) does not provide convincing evidence for the presence of rosettes in mammalian cells.

Since the extent to which the aggregation of intramembranous particles plays a role in phagocytosis is unknown, the aim of this study is to characterize the type and extent of intramembranous particle interactions during bacterial phagocytosis. The results of the freeze-fracture study are correlated with results of the thin-section and scanning electron microscope studies of the same membrane events. A preliminary report of this work was presented at the 1975 annual meeting of the American Society for Cell Biology (37).

MATERIALS AND METHODS

Selection of In Vitro Phagocytic System

Rabbit PMN leukocytes (heterophils, reference 70) were chosen for this study because Hirsch (23) has shown they can be obtained in reasonable quantities in nearly homogeneous populations from glycogen-induced peritoneal washes. In addition, rabbit PMN leukocytes have been thoroughly studied, and a great deal is known about their cell biology (25), development (4, 5, 69, 70), movement (24, 32), phagocytosis (24, 27, 50) ultrastructure (27, 33, 75), metabolism (43), lysosomal content (4, 27, 33, 74), and cytochemistry (4, 27, 69, 70).

Escherichia coli were selected for this study because their distinctive cell wall, cell shape, and membrane fracture faces make them easy to identify in freeze-fracture preparations. In addition, *E. coli* are readily available and easily maintained in the laboratory.

Leukocyte Isolation

Rabbit PMN leukocytes were obtained from peritoneal exudates according to the method of Hirsch (23). Briefly, this involved injecting healthy male New Zealand rabbits weighing 3–4 kg with 200–250 ml of sterile phosphate-buffered saline solution (PBS) containing 1 mg/ml of glycogen (Type 11, Sigma Chemical Co., St. Louis, Mo.). The cells were harvested after 4 h. The peritoneal wash fluid was centrifuged in the cold (4°C) for 10 min at 800 *g*. Then, the cell pellets were resuspended in Eagle's minimal essential culture medium (Eagle's MEM) at room temperature. An aliquot of cell suspension was removed and stained with Wright's stain. Only peritoneal washes that contained more than 95% PMN leukocytes were used. The cell concentration was determined by hemacytometer counts and adjusted to a final concentration of 2×10^6 cells/milliliter in the incubation medium.

The incubation medium consisted of Eagle's MEM culture medium (F-12, Grand Island Biological Co., Grand Island, New York) supplemented with heat-inactivated (50°C, 20 min) 15% rabbit serum (vol/vol), 0.01% bovine serum albumen, and 5 mM glucose. The leukocytes were then incubated at 37°C in a water bath.

Bacterial Preparation

Escherichia coli, strain K-12, W-3-110 wild type, were grown in trypticase soy broth and harvested in log phase growth. The bacterial cells were centrifuged (3,000 *g*) and resuspended in the previously described culture medium, to a final concentration of 2×10^7 to 2×10^8 cells per milliliter.

Phagocytosis Experiments

The design of the phagocytosis experiments was essentially the same as that of van Furth and van Zwet (74). Equal volumes of cells and bacteria were mixed to obtain a final concentration of 1×10^6 neutrophils per milliliter, and 1×10^7 to 1×10^8 bacteria per milliliter. These suspensions were incubated at 37°C, and experiments were performed at 0-, 3-, and 10-min intervals to determine the incubation time at which all of the different stages of phagocytosis were present. At 3-min incubation times, many of the different stages of phagocytosis were seen. The fixative used throughout these studies was a 2% glutaraldehyde fixative, buffered with 0.1 sodium cacodylate pH 7.2–7.4 at 37°C. This fixative provided good ultrastructural preservation of rabbit PMN leukocytes as judged by the preservation of lysosomes and other cytoplasmic constituents in thin sections (38).

SEM Preparations

Leukocytes were allowed to attach and spread on either glass or gold-coated glass substrates for at least 10 min at 37°C before the bacteria were added. In this way, we were able to separate those cell shape changes associated with substrate attachment from those changes associated with phagocytosis. After the cells had attached to the substrate, an equal volume of bacterial suspension was added to the cells to initiate phagocytosis.

The ratio of bacteria to leukocytes was between 10–100 bacteria per leukocyte. The same incubation media and temperature were maintained throughout these experiments. After 0, 3, and 10 min, unattached bacteria were gently rinsed from the leukocytes with fresh medium, and the cells were fixed for 1 h in the glutaraldehyde fixative at 37°C. After fixation, the cells were washed with 7% sucrose/0.1 M sodium cacodylate, pH 7.2 and then fixed for 1 h in 2% OsO_4 in 0.1 M cacodylate buffer, pH 7.2–7.4 at room temperature. Subsequently, an osmium-binding procedure was performed on the cells to increase their electrical conductivity in the SEM (29). Then, the cells were dehydrated in ethanol and critically point dried (1, 12) in a Bomar SPC/900 critical point apparatus (The Bomar Co., Tacoma, Wash.). The dried specimens were coated with a 10.0–20.0-nm layer of gold or gold-palladium in an EMS-41 minicoater (Film Vac. Incorporation, Englewood, N.Y.) and observed in a Coates and Welter, model 106, field emission scanning electron microscope.

Thin Section

Phagocytizing cells were fixed as described previously and stored overnight in 7% sucrose in 0.1 M cacodylate buffer 7.2 at 4°C. The cells were then fixed for 1 h in 2% OsO_4 in 0.1 M cacodylate buffer pH 7.2–7.4 at room temperature, dehydrated in ethanol, and embedded in Epon (34) which was then polymerized. Thin sections were cut with an LKB ultramicrotome (LKB Instruments, Rockville, Md.), picked up on uncoated copper grids, and stained with uranyl acetate and lead citrate (51). Electron micrographs of thin sections were taken with a Hitachi HU-12 electron microscope operated at 75 kV and calibrated with a carbon replica of an optical diffraction grating (E. F. Fullam, Inc., Schenectady, N.Y.).

Freeze-Fracture

Phagocytizing and nonphagocytizing leukocytes were fixed for 1 h in the previously mentioned fixative, centrifuged at 500 *g* for 10 min and resuspended in either 20% or 30% aqueous glycerol solution (vol/vol).

After overnight equilibration in the cold, the cells were gently centrifuged (500 *g*, 10 min) and a dense cell suspension was loaded into gold specimen holders. The holders were then rapidly frozen in resolidifying

Freon-12 (−150°C). Excess liquid freon was quickly blotted off the holders without warming, and the holders were cooled to liquid nitrogen temperature (−196°C). The specimen holders were loaded into a precooled Denton DFE-2 freeze-etching unit (Denton Vacuum Inc., Cherry Hill, N.J.) mounted on a Varian FE-12 high pumping vacuum station Varian Associates, Palo Alto, Calif.). With this vacuum system, an oil-free vacuum of better than 1×10^{-7} Torr was obtained within 5 min of specimen insertion. The vacuum system and the electrode assemblies used in the freeze-etch unit are described in detail elsewhere (7). The cells were freeze-fractured at −125°C ± 5°C and replicated immediately esentially according to Steere's recommendations (59). After replication, the holders were removed from the vacuum system, and replicas were floated off the gold holders onto the surface of 15% sodium hypochlorite in distilled water. Adhering biological material was dissolved from the replicas with aqueous sodium hypochlorite solutions of increasing concentrations. After cleaning, the replicas were rinsed on the surface of distilled water and picked up on Formvar-coated grids. The freeze-fracture replicas were examined in a Hitachi HU-12 transmission electron microscope at 75 kV calibrated as described previously.

Measurements and Counts of IMPs

REPLICA RESOLUTION: In this study, only replicas exhibiting high resolution were used for counting and measuring intramembranous particles. Replicas of low or moderate resolution gave lower counts of intramembranous particles probably because some of the smaller IMPs could not be resolved in these replicas. Pinto da Silva and Miller (47) have noted a similar effect of replica resolution on IMP detection in myelin membranes. The freeze-fracture terminology used in this report conforms to the nomenclature proposed for freeze-fractured membranes (9).

MEASUREMENTS: All electron micrographs of freeze-fractured membranes were photographed at × 50,000 and printed at a final magnification of 100,000, i.e., 100 nm = 1 cm. Then, a grid pattern with X and Y coordinates and millimeter divisions was taped securely over the micrograph which was mounted on a light box. Intramembranous particles were then measured, counted, and immediately marked with a pencil to eliminate the possibility of counting or measuring the same particle twice.

The size of the intramembranous particles were measured with a calibrated ocular micrometer. They were measured across their "diameters" in a direction perpendicular to the direction of shadow to the nearest 0.1 mm. Then the size of an IMP was recorded on a frequency chart in which the X, Y coordinates of the 0.01 μm^2 square were also recorded. The tabulation of data in this form facilitated analysis and permitted simplified checking of data.

RESULTS

Scanning Electron Microscopy

Neutrophils normally exhibit a variety of different cell shapes, regardless of whether they are phagocytizing bacteria or not. In general, phagocytizing cells appear rounder with smaller membrane extensions than cells that are not engulfing bacteria.

During phagocytosis, the initial attachment of bacteria appears to occur randomly on the leukocyte surface. That is, no preferred site for attachment is seen in our preparations. In phagocytizing cells, membrane-bound extensions are frequently seen at, or in, the immediate vicinity of attached bacteria (Figs. 1 and 2). The size and shape of the initial attachment site varies with the size, shape, and orientation of the bacteria (Figs. 1 and 2). Consequently, the estimated area of initial contact between a leukocyte and a bacterium ranged in size from about 0.01 to 0.25 μm^2 (Fig. 1). Once a substantial portion of the membrane folds surrounded the bacterium, it became more difficult to estimate the extent of membrane-surface that was in direct contact with the bacteria.

During phagocytosis, small spherical shapes are seen on the leukocyte cell surface (Fig. 2). These are believed to represent the exocytosis of lysosomal contents into the external medium that is known to occur during phagocytosis (73).

After ingesting bacteria, leukocytes are more spherical in shape and have smaller membrane-bound extensions. In addition, only the outlines of the engulfed bacteria are seen on the cell surface (Fig. 3).

Thin Sections

The ultrastructural preservation of PMN leukocytes in each peritoneal wash was assessed with thin-section techniques. As we reported previously (38), the characteristic primary (azurophil) and secondary (specific) lysosomes, as well as phagocytic vacuoles of PMN leukocytes, appear to be well preserved in our preparations. Typical images characteristic of the different membrane events in phagocytosis were obtained. These images are similar to those previously reported by others (27, 33, 75), and are included here only as an aid in interpreting the three-dimensional aspects of SEM and freeze-fracture ultrastructure.

At the bacterial attachment site, a variety of membrane configurations were observed in thin sections. In some instances, the cross-sectional

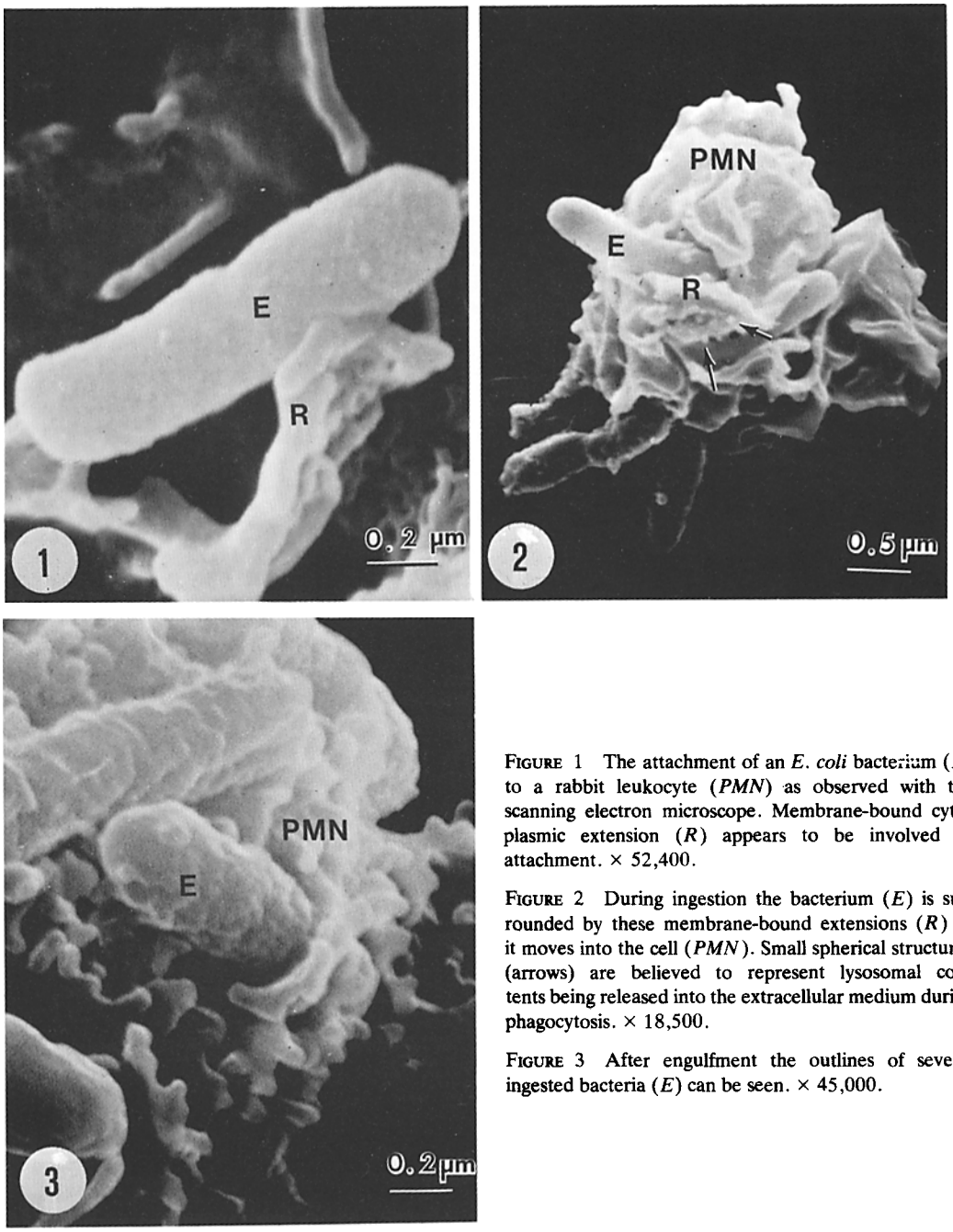

FIGURE 1 The attachment of an *E. coli* bacterium (*E*) to a rabbit leukocyte (*PMN*) as observed with the scanning electron microscope. Membrane-bound cytoplasmic extension (*R*) appears to be involved in attachment. × 52,400.

FIGURE 2 During ingestion the bacterium (*E*) is surrounded by these membrane-bound extensions (*R*) as it moves into the cell (*PMN*). Small spherical structures (arrows) are believed to represent lysosomal contents being released into the extracellular medium during phagocytosis. × 18,500.

FIGURE 3 After engulfment the outlines of several ingested bacteria (*E*) can be seen. × 45,000.

thickness of membranes at the attachment site could be seen (Fig. 5). A symmetrical arrangement of membranes was occasionally seen at the attachment site of a bacterium. This symmetry was due to the relatively constant 33-nm spacing between the leukocyte membrane and bacterial cell wall (Figs. 4 and 5). The bacterial cell wall itself measured 10–14 nm thick and consisted of three layers: an inner layer which measured 6–8 nm and two outer layers each 2–4 nm in thickness. In addition, the opsonized bacteria were coated with an electron-dense layer of material about 14

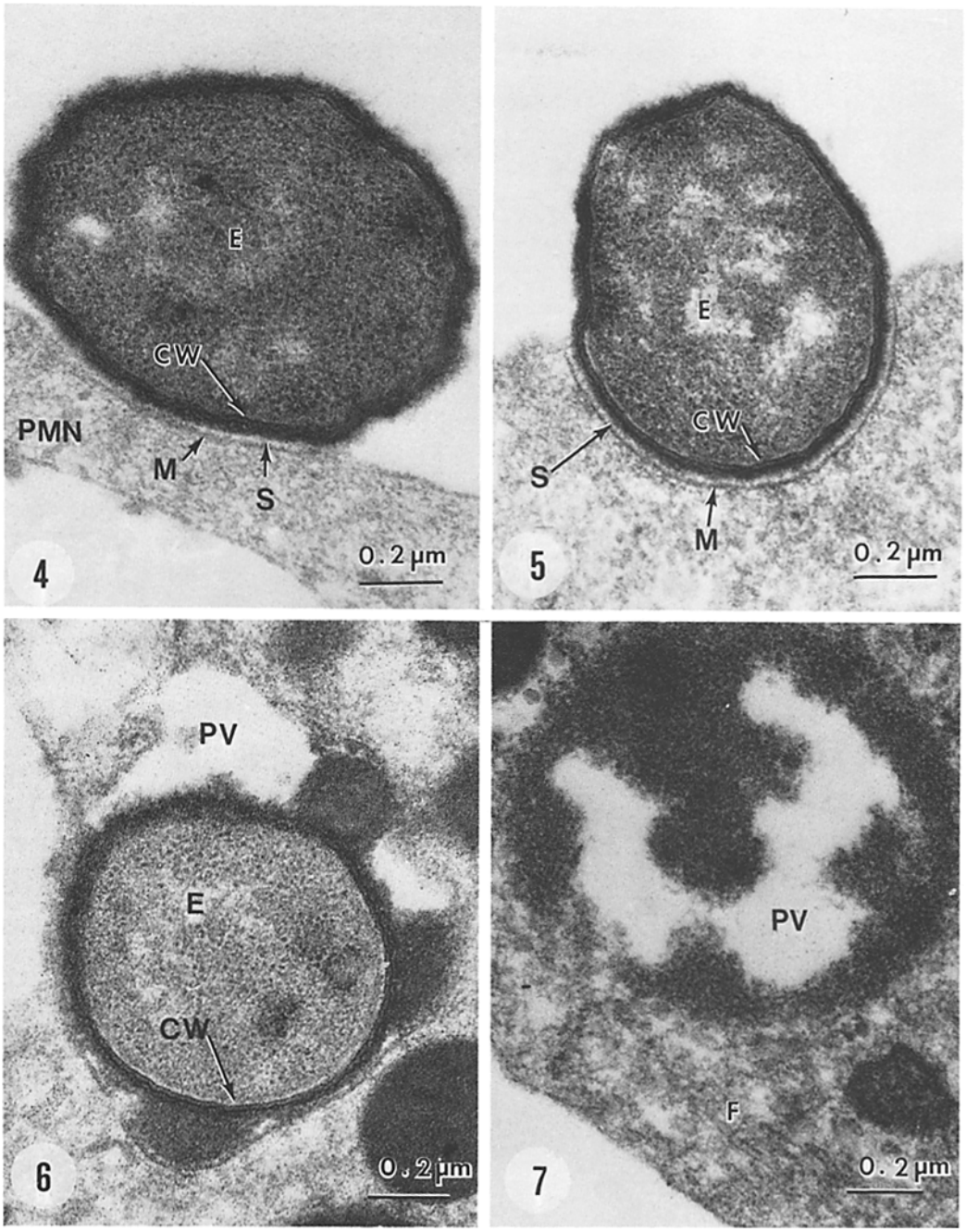

FIGURE 4 The attachment of an *E. coli* (*E*) to a rabbit polymorphonuclear leukocyte (*PMN*) as observed in a thin section. At this early stage of phagocytosis the bacterial wall (*CW*) and the leukocyte membrane (*M*) are separated by a distance (*S*) of about 33 nm. × 60,000.

FIGURE 5 The ingestion of an *E. coli* (*E*) showing the membrane systems involved in its engulfment. A relatively constant spacing of 33 nm (*S*) between the leukocyte membrane (*M*) and the bacterial cell wall (*CW*) is maintained during ingestion. × 60,000.

FIGURE 6 This figure shows a phagocytic vacuole (PV) at an early stage of lysosomal fusion with the phagocytic vacuole. The bacterial cell wall (*CW*) is still intact. × 60,000.

FIGURE 7 After ingestion the *E. coli* is digested within the phagocytic vacuole (*PV*) by lysosomal action. A bundle of filaments (*F*) lies near the phagocytic vacuole (*PV*). The bacterial cell wall is no longer apparent. × 60,000.

nm thick. The rabbit PMN plasma membrane was 7 nm thick.

After ingestion of the *E. coli,* lysosomal and phagocytic vacuoles fused. (Figs. 6 and 7). Cell suspensions allowed to phagocytize bacteria for 10 min showed evidence of considerable degranulation, i.e., the release of lysosomal contents into phagocytic vacuoles, and disruption of the bacterial cell (Fig. 7). It was more difficult to clearly identify the phagocytic vacuoles in these preparations (Fig. 7).

Bundles of microfilaments similar to those previously reported to be associated with rabbit PMN lysosomes (38) were also observed near phagocytic vacuoles (Fig. 7).

Freeze-Frature

The process of phagocytosis as seen in freeze-fracture images corresponds well to that seen in thin-section and SEM preparations (cf. Figs. 8–10 with Figs. 1–3 and 4–7). In addition, the results with freeze-fracture yield new information on the internal structure of membranes during phagocytosis.

In this study, the two fracture faces of PMN leukocyte plasma membranes were distinguished by their different densities of intramembranous particles per square micrometer. In high resolution replicas, the protoplasmic fracture face (PF) has 1,878 particles per square micrometer while the extracellular fracture face (EF) had 906 particles per square micrometer (Figs. 11 *a* and *b* and Table I).

By inspection, it is possible to see that phagocytizing and nonphagocytizing cells show little difference in the number or size distribution of intramembranous particles on either the PF- or EF-fracture faces (Figs. 11 *a* and *c*; and 11 *b* and *d*). Fig. 12 shows the total number of IMPs per square micrometer of each fracture face shown in Fig. 11. The mean and standard deviation for each of these populations are given in Table I. Fig. 13 shows a frequency distribution of the IMP size of both the PF- and EF-fracture faces shown in Fig. 11 *c* and *d*.

It is apparent that a massive aggregation of intramembranous particles does not occur in either phagocytizing or nonphagocytizing plasma membranes (Figs. 11 *a–d*, and Figs. 14 *a* and *b*). Furthermore, no unusual aggregations of intramembranous particles were observed in membrane extensions of PMN plasma membranes (Fig. 15; see Table II). However, several qualitative changes in the distribution of IMPs were seen in phagocytizing plasma membranes. These will be presented in more detail below.

The azurophil and specific lysosomes were recognized in freeze-fracture replicas by their size and shape (6, 17, 42). The azurophil lysosomes (Fig. 16 *a*) were usually more spherical and larger (0.5–0.8 μm diameter) than specific lysosomes (0.3–0.5 μm in their longest dimension). Specific granules are also more elongate in shape (Fig. 16 *b*). The lysosomal membranes of both azurophil and specific granules contain intramembranous particles, which suggests that they may also contain membrane-bound proteins or glycoproteins. This thinking is consistent with recent lectin-binding studies and biochemical studies which suggest that carbohydrate moieties (17), membrane-bound proteins (13) and glycoproteins (42) are present in lysosomal membranes. The density of intramembranous particles in lysosomal membranes appears to be similar to that seen in the other leukocyte membranes (Fig. 16 *a* and *b*; Table II).

Fractures through phagocytizing PMN plasma membranes exactly at the bacterial attachment site were observed (Fig. 14). Although it was often difficult to discern the membrane structure immediately beneath the bacteria, fractures through the plasma membrane in the immediate vicinity of attached bacteria usually revealed little or no aggregation of intramembranous particles (Figs. 8 and 14 *b*). However, certain changes in the distribution of IMPs were seen in membranes involved in phagocytosis. These changes included: (*a*) a limited clustering of IMPs in the immediate vicinity of some (but not all) bacterial attachment sites (cf. Fig. 14 *a* and *b*), and (*b*) the occasional presence of IMP-free regions which we believe represent sites of membrane fusion between lysosomal and plasma membranes (Figs. 2 and 8). We believe these structural changes are representative of the membrane fusion associated with lysosome release which is known to occur during phagocytosis (73) and other stimulatory events (15, 22, 40, 53, 56).

Phagocytic vacuole membranes were identified as those cytoplasmic membranes which completely enclosed cross-fractured *E. coli* (Figs. 17 *a, b,* and 18). In the initial stages of phagocytosis, phagocytic vacuole and plasma membranes had intramembranous particles with a similar distribution and density (Table II).

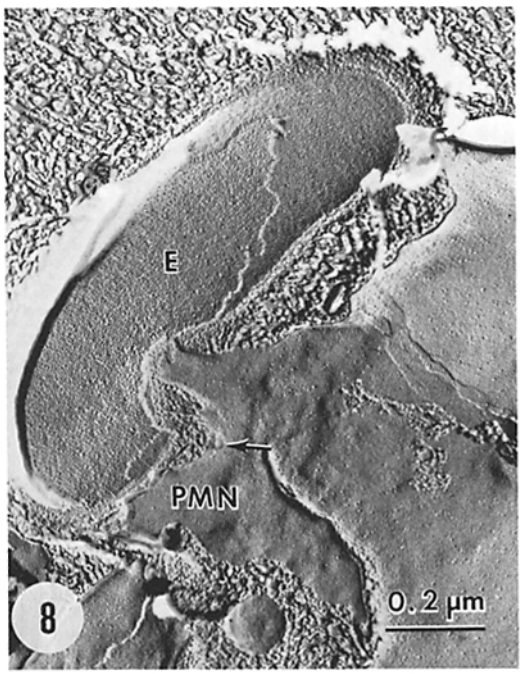

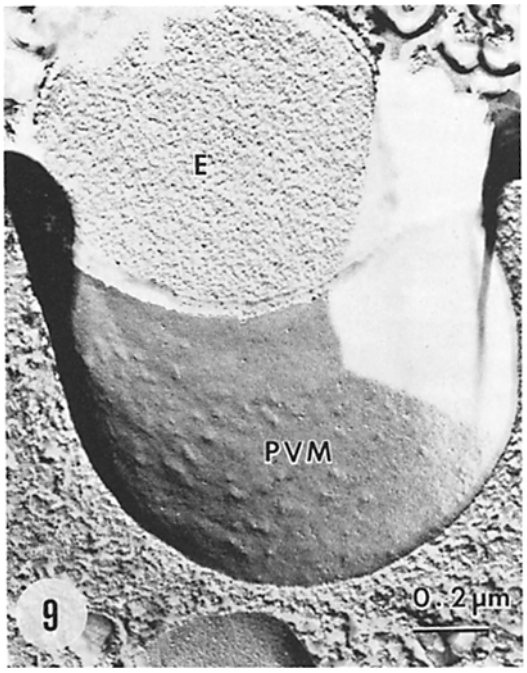

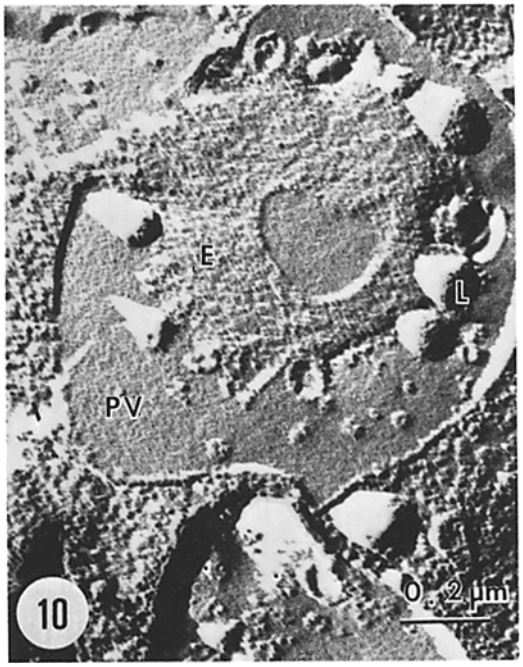

FIGURE 8 During attachment intramembranous particles (IMP) are seen within freeze-fractured leukocyte (*PMN*) plasma membranes. In general, the distribution of these particles within does not appear to drastically change during bacterial attachment. However, small changes in IMP distribution are seen. These include the development of IMP-free regions within the membrane (arrowhead) and small aggregations of IMP in the vicinity of some bacteria (see Fig. 14 b). × 27,400.

FIGURE 9 During ingestion, the formation of the phagocytic vacuole begins. Early phagocytic vacuole membranes (*PVM*) resemble the plasma membranes in the size, number, and distribution of intramembranous particles. × 60,000.

FIGURE 10 After ingestion and lysosomal action, disrupted bacterium, *E. coli* (*E*), and remnants of lysosomes (*L*) are found within the phagocytic vacuole (*PV*). Cf. Figs. 7 and 8. × 60,000.

A lower density of intramembranous particles was seen in some of the later stages of phagocytosis. However, the values did not fall substantially below the count for a normal EF face of the plasma membrane (Table II). Thus, it was not possible to decide if the IMP count actually decreased, even though a decrease might be expected if lytic enzymes attacked these IMPs (16).

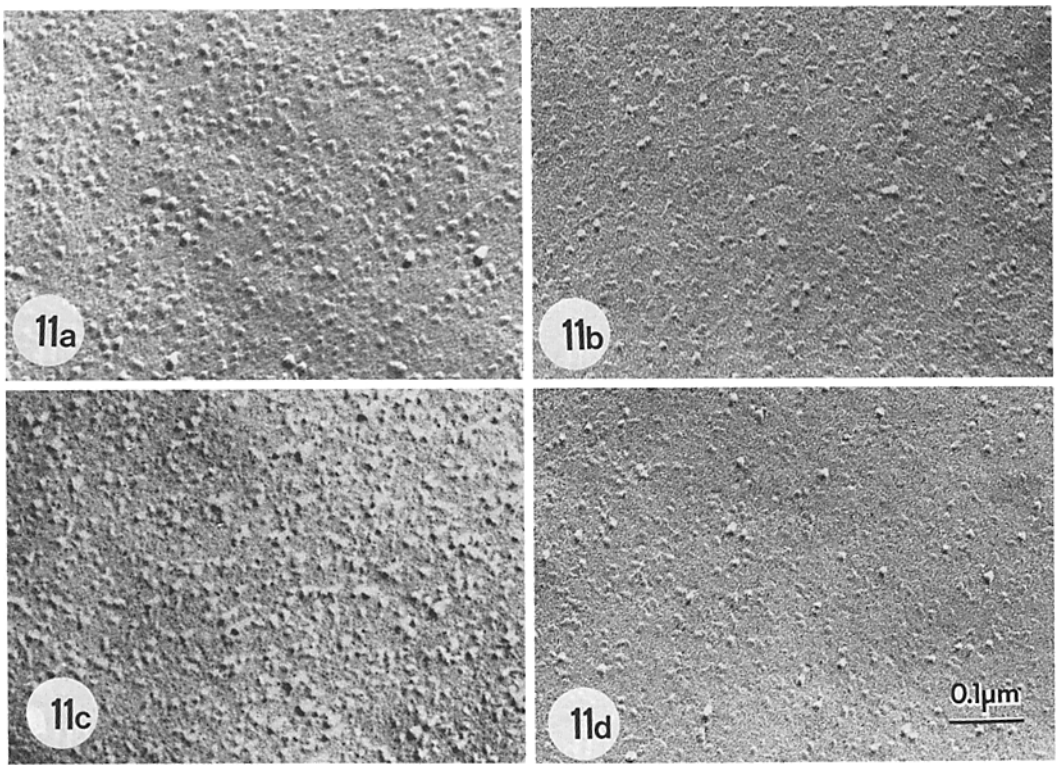

FIGURE 11 Freeze-fractured PMN plasma membranes appear to have two fracture faces. In these figures the protoplasmic fracture face (PF) has about twice as many intramembranous particles (IMP) per square micrometer as the extracellular fracture face (EF). Figs. 11 *a* and *b* are from a nonphagocytizing cell, while Figs. 11 *c* and *d* are from a phagocytizing cell. × 100,000.

TABLE I

IMP Density and Aggregation in Neutrophil Plasma Membranes*

Plasma membranes		IMP‡			IMP aggregation
		Counts/μm²	*SD§/μm²*	*SEM‖/μm²*	
Not phagocytising	PF	1,878	359	50	None
	EF	906	293	41	None
Phagocytising	PF	1,520	327	46	Little or none
	EF	1,122	291	41	None

This table summarizes our observations on the density and state of aggregation of IMPs in the plasma membrane of rabbit PMN (heterophil) leukocytes.

* Neutrophil refers to rabbit PMN (heterophil) leukocyte.

‡ The values for these counts are taken directly from 0.5 μm areas of each of Figs. 11 *a–d*.

§ The SD was calculated for an area of 0.5 μm in a high resolution replica, where the variate, x, equalled the number of IMPs/0.01 μm^2.

‖ The SEM was calculated with SD data and results and is also based on the variate, x, the number of IMPs/0.01 μm^2.

After longer time intervals (10 min), lysosomal action made it more difficult to clearly identify phagocytic vacuoles because the bacteria lost their structural integrity (cf. Figs. 7 and 10).

Shortly after ingestion, local changes in phagocytic vacuole membranes were seen. Intramembranous particles were occasionally aligned in rows within the phagocytic vacuole membranes (Figs. 17 *a* and *b*).

In the later stages of phagocytosis, sites of mem-

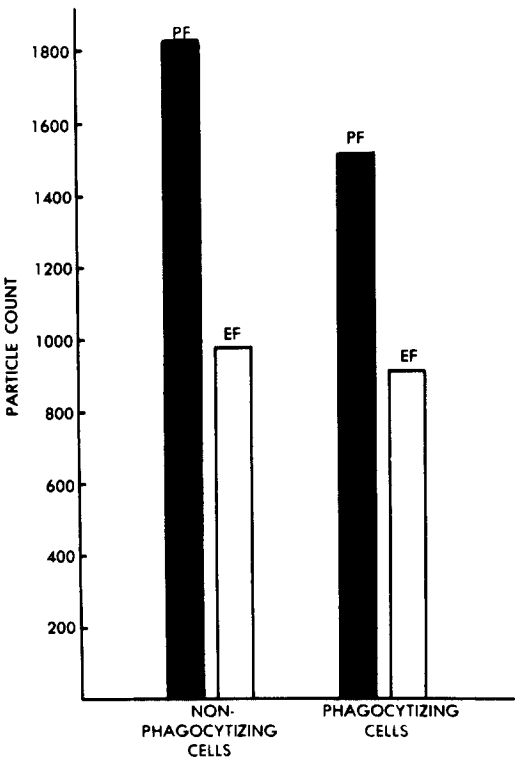

FIGURE 12 This histogram compares the size distribution of intramembranous particles from 1-μm^2 areas of the extracellular (*EF*) and protoplasmic (*PF*) fracture faces of nonphagocytizing cells. (See Figs. 11*a* and *b*).

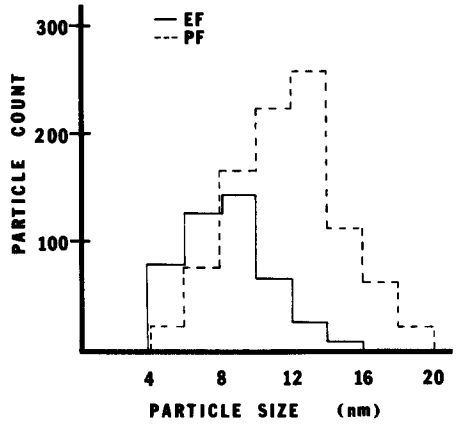

FIGURE 13 This histogram compares the number of IMP per square micrometer of membrane surface of the extracellular fracture face (*EF*) with that of the protoplasmic fracture face (*PF*) of phagocytizing and nonphagocytizing rabbit leukocytes. Data taken from Figs. 11*a–d*.

brane fusion between phagocytic vacuoles and lysosomes were seen (Fig. 18). These fusion sites appeared as small, irregularly shaped "holes" in the normally intact membrane fracture faces of the phagocytic vacuole (cf. Figs. 17 and 18). Thus far, no rosette patterns of intramembranous particles have been observed at or near these fusion sites in either phagocytizing rabbit PMN leukocytes or those treated with calcium and the divalent ionophore A23187 to induce lysosomal membrane fusion and release (40).

DISCUSSION

In this paper, we have demonstrated the sequence of membrane events that occur within leukocyte membranes during phagocytosis. Our results suggest that intramembranous particles are distributed asymmetrically across PMN plasma membranes, and that a massive aggregation of intramembranous particles does not occur during bacterial phagocytosis. Instead, local changes occur within the membranes of phagocytizing cells. These local changes include: (*a*) the alignment of intramembranous particles into linear arrays in newly formed phagocytic vacuole membranes, (*b*) the lateral displacement of intramembranous particles at the sites of membrane fusion between lysosomal and phagocytic vacuole membranes, and (*c*) the occasional clustering of small groups of intramembranous particles near bacterial attachment sites. These clusters are neither so symmetrically arranged nor so frequently found as those in protozoan membrane fusion (52). In addition to changes in membrane structure during phagocytosis, changes in cell shape also occur. PMN leukocytes tend to change from flattened, extended shapes to more spherical shapes. Simultaneously, there is a reduction in the size of membrane extensions as phagocytosis proceeds. These cell shape changes are probably the result of structural and functional changes in both the contractile elements (21, 28, 30, 39, 60, 61, 62, 63) and the membrane systems present in these nonmuscle cells.

It is worthwhile to compare PMN leukocyte membranes with the more extensively studied erythrocyte membranes. Like erythrocyte membranes (67, 68), leukocyte membranes appear to have two fracture faces and an asymmetric distribution of IMPs across the lipid bilayer, but the total number of IMPs μm^2 on the respective PF- and EF-fracture faces is lower for leukocyte membranes.

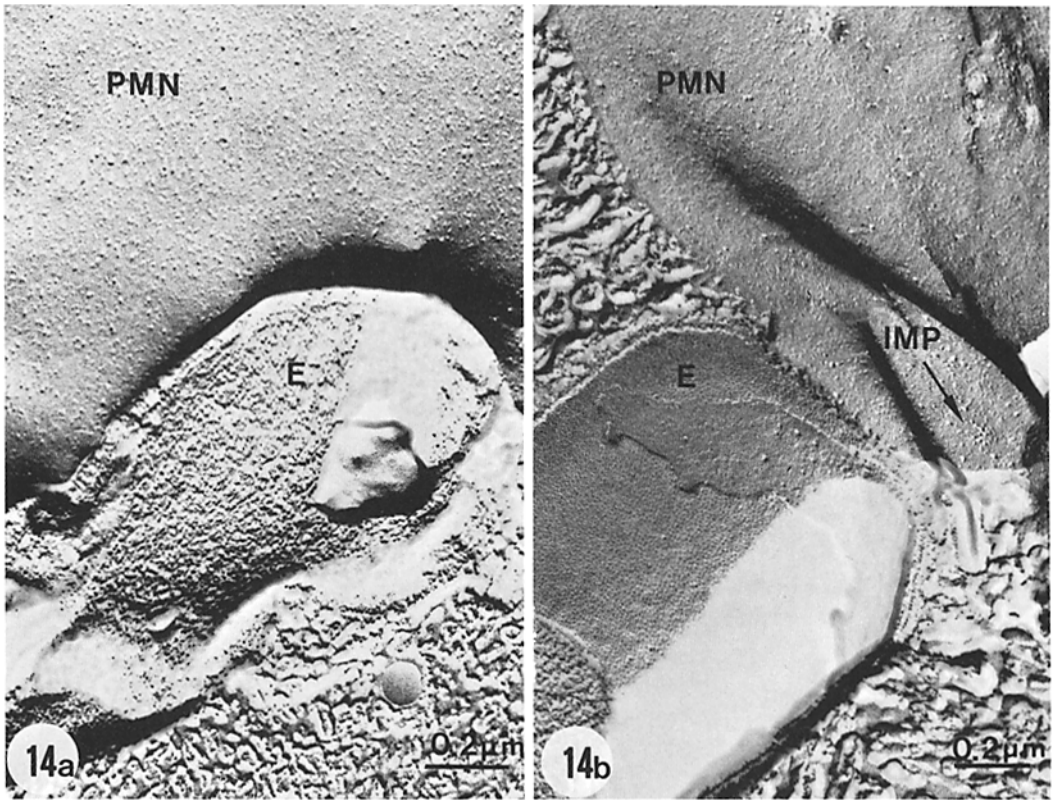

FIGURE 14 These electron micrographs demonstrate small clusters of intramembranous particles (*IMP*) in the vicinity of some but not all attached bacteria (*E*). Fig. 14 *b* shows particles aggregated into small clusters (*IMP*), while aggregated particles are not seen in Fig. 14 *a*. × 55,200.

It is thought that erythrocyte IMPs represent sites for receptor binding since the binding of viruses (64), divalent antibody (46), and plant lectins (64) aggregate IMPs. In addition, it is thought that erythrocyte IMPs might be attached either directly or indirectly to a submembranous network of spectrin and actin (14, 58, 65), and that interactions within this network (8, 14, 55, 65) control the shape of erythrocytes. Much less is known about the possible roles of IMP aggregation in PMN leukocytes. When IMPs aggregate in leukocyte membranes during phagocytosis, it is at most a local response and not a cell-wide phenomena as it is in erythrocyte ghost membranes (14, 44) and in virally fused cells (2, 3). Furthermore, since a spectrinlike molecule has not been isolated from PMN leukocytes, it is not known if a spectrin-actin network is responsible for leukocyte cell shape transformation. It is possible that erythrocytes and leukocytes control cell shape and membrane interactions in different ways. Recent evidence suggests that high molecular weight proteins (21, 28, 61) and/or low molecular weight (35, footnote 1) proteins control the physical state of actin gels in leukocytes which in turn may be partially responsible for cell shape transformations and perhaps the movements of lysosomes (38, 40).

The SEM observations during phagocytosis indicate that bacteria can attach at any point on the leukocyte cell surface, and that membrane extensions are frequently involved in the process of contacting, attaching, and ingesting bacteria. The findings with freeze-fracture indicate that there is no specialized structural feature of intramembran-

[1] Condellis and Taylor have recently demonstrated a calcium-sensitive transition of cytoplasmic gels to "sols" in motile extracts of *Dictyostelium* (*J. Cell Biol.* 1977. **74**:901–927). This observation may have important implications in lysosomal movements, if similar results are obtained in mammalian cells.

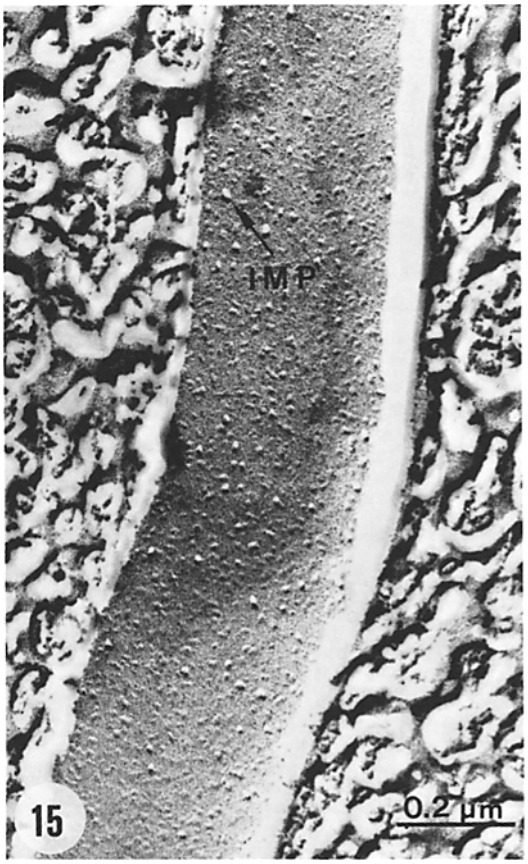

FIGURE 15 No unusual aggregation of intramembranous particles (*IMP*) was observed within the membrane-bound cytoplasmic extensions of PMN leukocyte. × 78,800.

ous particles in these membrane-bounded extensions. Our results support the contention suggested by others that membrane extensions provide a reservoir of extra membrane surface that becomes part of the phagocytic vacuoles during phagocytosis (20). The loss of this available surface area might regulate the cell shape changes that occur during phagocytosis, and perhaps also the number of bacteria that can be engulfed.

Bacterial attachment does not appear to cause a cell wide aggregation of intramembranous particles like that seen in erythrocyte ghost membranes during a variety of treatments. Instead, our results suggest that, if bacterial attachment produces a change in the structure of the plasma membrane, this change is a local response limited primarily to regions of direct contact between leukocytes and bacteria.

The formation of phagocytic vacuoles from the plasma membrane involves not only the inward movement of the lipid bilayer but also the inward movement of intramembranous particles along with the lipid bilayer. The movement of IMPs into phagocytic vacuole membranes could be the result of a simple diffusion of IMPs in a fluid membrane (18, 57) or a more complex interaction of membranes and membrane-associated proteins (8, 14, 55, 56, 66).

The appearance of aligned IMPs within early phagocytic vacuole membranes suggests that linear elements such as cytoplasmic microfilaments or microtubules might interact either directly or indirectly with the phagocytic vacuole membrane on its cytoplasmic surfaces. The explanation why these arrangements are not observed in all phagocytic vacuoles or on all parts of the plasma membrane remains to be elucidated. Several possible explanations exist. For example, since phagocytosis occurs so rapidly (25), only a few such interactions might be expected to be seen at any one time. Alternatively, other conditions such as the ionic environment (63) might regulate such interactions in the vicinity of phagocytic vacuoles.

The fusion of lysosomal and phagocytic vacuole membranes appears to be different from that observed in *Tetrahymena* mucocyst secretion (52) since highly symmetrical aggregations of IMPs are not seen in phagocytizing leukocytes. Rosettes are also lacking during membrane fusion induced with the divalent ionophore A23188 and extracellular calcium. This treatment induces the fusion of lysosomes with the plasma membrane (40) and the release of lysosomal enzymes into the extracellular medium (15, 19). The formation of IMP-free regions during ionophore A23187-induced fusion of the lysosomal membrane with the plasma membrane resembles that seen during phagocytosis, protozoan membrane fusion (52), and other types of mammalian membrane fusion (10, 11, 31). At present, the formation of these IMP-free regions appears to be the most universal structural feature of membrane fusion.

The observation that rabbit PMN lysosomal membranes, like Chediak-Higashi PMN lysosomal membranes (71), contain IMPs is interesting since it suggests that these membranes are more structurally complex than was previously thought. It seems likely that lysosomal IMPs are composed, at least in part, of glycoproteins since these membranes contain proteins (13) and glycoproteins (42) and since plant lectins bind to

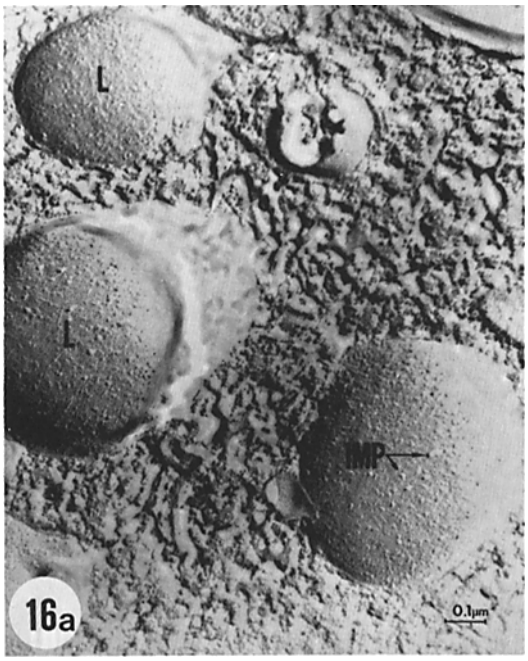

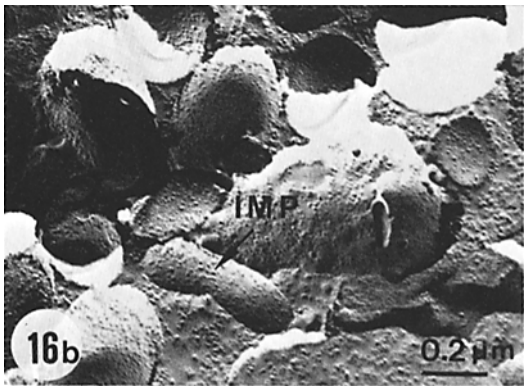

FIGURE 16 (*a* and *b*) Intramembranous particles were observed on the fracture faces of azurophil (Fig. 16 *a*) and specific (Fig. 16 *b*) lysosomal membranes in non-phagocytizing neutrophils. (*a*) × 55,400; (*b*) × 41,900.

TABLE II

IMP Density and Aggregation in Neutrophil Organelle Membranes*

Organelle membranes	IMP			IMP aggregation
	counts/μm²	*SD‡/μm²*	*SEM§/μm²*	
Membrane extensions of plasma membrane	1,397	334	66	None
	1,193	340	44	
Lysosomal membranes (not phagocytizing)	1,260	337	107	None
	1,040	251	112	
Phagocytic vacuole membranes (without lysosomal fusion)	2,180	228	102	None, but occasional aligned IMP visible.
	1,225	354	125	
	1,000	272	72	
Phagocytic vacuole membranes (lysosomal fusion apparent)	890	292	92	None, but "fusion sites" visible.

This table summarizes our observations on the density and state of aggregation of intramembranous particles in the organelle membranes of rabbit PMN (heterophil) leukocytes.

* Neutrophil refers to rabbit PMN (heterophil) leukocyte.

‡ SD equals Standard Deviation. Calculated for areas between 0.05 and 0.30 μm^2, where the variate, x, equalled the number of IMPs in a 0.01-μm^2 area.

§ Calculated with SD data and results on the number of IMPs in a 0.01 μm^2 area.

carbohydrate moieties on their cytoplasmic surfaces (17). The function of IMPs in lysosomal membranes is not known, but they might serve some receptor function on the cytoplasmic side of the membrane.

In conclusion, the value of this study is that it provides an initial characterization of the structural changes in leukocyte membranes during phagocytosis. The experimental system and conditions represent those commonly used in in vitro studies of phagocytosis and those that are believed to represent physiological conditions for leukocyte

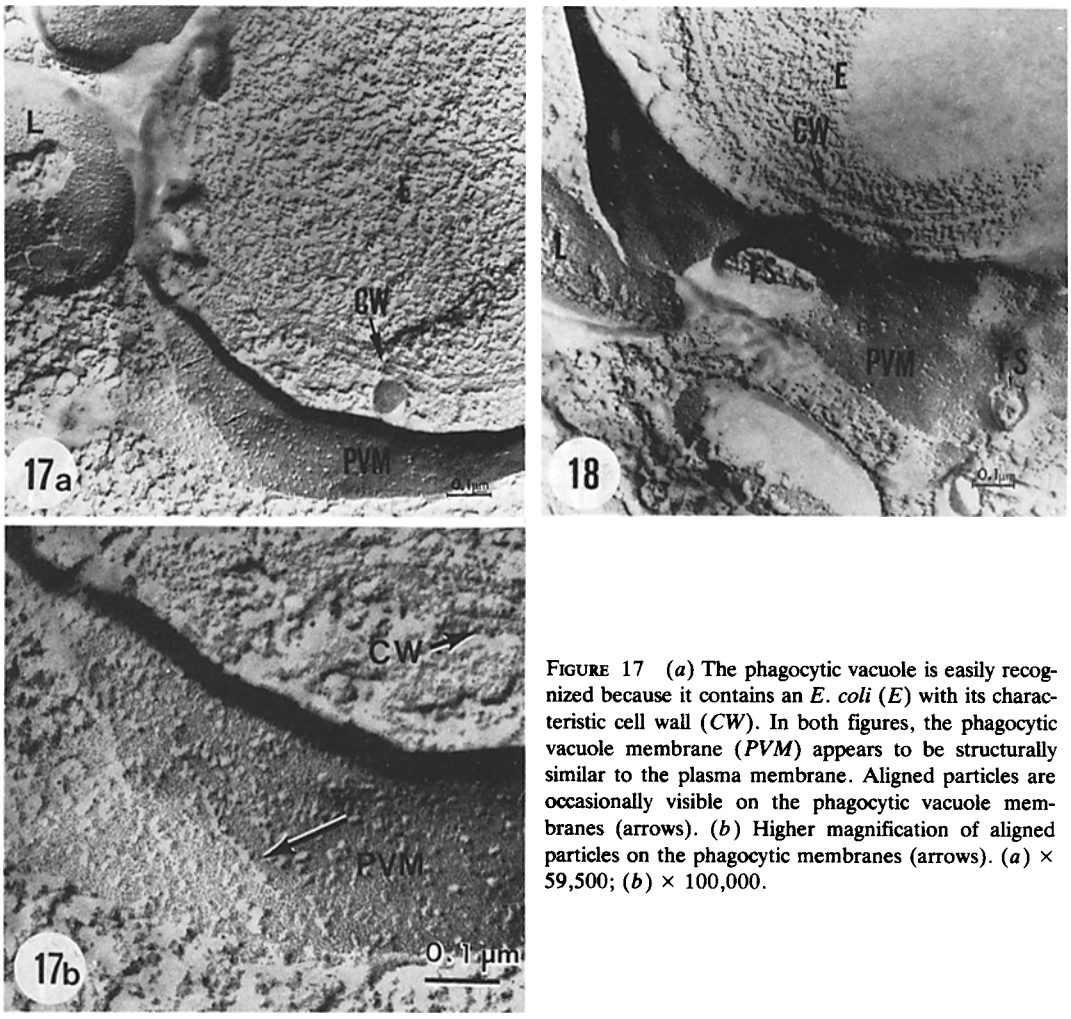

FIGURE 17 (*a*) The phagocytic vacuole is easily recognized because it contains an *E. coli* (*E*) with its characteristic cell wall (*CW*). In both figures, the phagocytic vacuole membrane (*PVM*) appears to be structurally similar to the plasma membrane. Aligned particles are occasionally visible on the phagocytic vacuole membranes (arrows). (*b*) Higher magnification of aligned particles on the phagocytic membranes (arrows). (*a*) × 59,500; (*b*) × 100,000.

FIGURE 18 Small irregularly shaped regions appear in the phagocytic vacuole membranes. These regions probably represent fusion sites (*FS*) between lysosomal membranes (*L*) and phagocytic vacuole membranes (*PVM*). × 55,600.

phagocytosis. The information obtained in this study should provide a useful guide for assessing the structural changes between naturally occurring membrane events and those that occur in membrane model systems. In addition, this information should prove valuable in the study of membrane receptors.

The authors thank Juliet Lilga, Ellie Setser, and Kathryn Hargrove for technical assistance; Fran Cameron, Karen Beaufort, and Norma Bendt at the Medical University of South Carolina, and Elizabeth Tartagni at Yale University Medical School for secretarial assisstance; Katherine King for editorial assistance; Jim Nicholson and Jim Scoggins for assistance in preparation of micrographs; Felix Rogers for use of his Normarski differential interference microscope; and Bill Greene and Dr. Douglas Balentine for use of their transmission electron microscope facilities. We are particularly grateful to Dr. Gordon R. Hennigar, Professor and Chairman, Pathology Department, Medical University of South Carolina, for his encouragement and support throughout the course of this project.

This work was supported by National Institutes of Health grants AM-10956 and AM-11028 to Dr. Sam S. Spicer and a training grant from Smith, Kline and French Laboratories, Philadelphia, Pennsylvania. The final revisions of this manuscript were made while Patrick L. Moore was supported by a National Institutes of Health postdoctoral fellowship no. AM-07107 in the

Department of Internal Medicine, Yale University School of Medicine and the Biology Department, Yale University.

Reprint requests should be sent to Dr. H. Bank in Charleston, South Carolina.

Received for publication 24 March 1976, and in revised form 19 August 1977.

REFERENCES

1. ANDERSON, T. F. 1951. Techniques for the preservation of three-dimensional structure for electron microscopy. *Trans. New York Acad. Sci.* **13:**130–150.
2. APOSTOLOV, K., and G. POSTE. 1972. Interaction of Sendai virus with human erythrocytes. A system for the study of membrane fusion. *Microbiology (Engl. Transl. Mikrobiologiya)* **6:**247–261.
3. BÄCHI, T. H., M. AGUET, and C. HOWE. 1973. Fusion of erythrocytes by Sendai virus studied by immuno-freeze-etching. *J. Virol.* **11:**1004–1012.
4. BAINTON, D. F., and M. E. FARQUHAR. 1968. Differences in enzyme content of azurophil and specific granules of polymorphonuclear leukocytes. I. Histochemical staining of bone marrow smears. *J. Cell Biol.* **39:**286–298.
5. BAINTON, D. F., and M. G. FARQUHAR. 1968. Differences in enzyme content of azurophil and specific granules of polymorphonuclear leukocytes. II. Cytochemistry and electron microscopy of bone marrow cells. *J. Cell Biol.* **39:**299–317.
6. BAGGIOLINI, M., J. G. HIRSCH, and C. DE DEUVE. 1969. Resolution of granules from rabbit heterophil leukocytes into distinct populations by zonal sedimentation. *J. Cell Biol.* **40:**529–541.
7. BANK, H., and J. D. ROBERTSON. 1976. A simple electrode for metallic replication. *J. Microsc. (Oxf.).* **106:**343–350.
8. BIRCHMEIR, W., and S. J. SINGER. 1977. On the mechanism of ATP-induced shape changes in human erythrocyte membranes. II. The role of ATP. *J. Cell Biol.* **73:**647–659.
9. BRANTON, D., S. BULLIVANT, N. B. GILULA, M. J. KARNOVSKY, H. MOOR, K. MÜHLETHALER, D. H. NORTHCOTE, L. PACKER, B. SATIR, P. SATIR, V. SEPTH, L. A. STAEHELIN, R. L. STEERE, and R. S. WEINSTEIN. 1975. Freeze-etching nomenclature. *Science (Wash. D. C.).* **190:**54–56.
10. BURWEN, S. J., and B. H. SATIR. 1977. A freeze-fracture study of early membrane events during mast cell secretion. *J. Cell Biol.* **73:**660–671.
11. CHI, E. Y., D. LAGUNOFF, and J. K. KOEHLER. 1976. Freeze-fracture study of mast cell secretion. *Proc. Natl. Acad. Sci. U. S. A.* **73:**2823–2827.
12. COHEN, A. L. 1974. Critical point drying. *In*: Principles and Techniques in Scanning Electron Microscopy. M. Hyatt, editor. Van Nostrand Reinhold Company, New York, NY. 44–112.
13. DEWALD, B., R. RINDER-LUDWIG, U. BRETZ, and M. BAGGIOLINI. 1975. Subcellular localization and heterogeneity of neutral proteases in neutrophilic leukocytes. *J. Exp. Med.* **141:**709–723.
14. ELGAESTER, A., D. M. SHOTTEN, and D. BRANTON. 1976. Intramembrane particle aggregation in erythrocyte ghosts. II. The influence of spectrin aggregation. *Biochim. Biophys. Acta.* **426:**101–122.
15. ESTENSEN, R. D., M. E. REUSCH, M. L. EPSTEIN, and H. R. HILL. 1976. Role of Ca^{2+} and Mg^{2+} in some human neutrophil functions as indicated by ionophore A23187. *Infect. Immun.* **13:**146–151.
16. ENGSTROM, L. H. 1970. Structure in the erythrocyte membrane. Ph.D. Dissertation. University of California, Berkeley, Calif.
17. FEIGENSON, M. E., H. P. SCHNEBLI, and M. BAGGIOLINI. 1975. Demonstration of ricin-binding sites on the outer face of azurophil and specific granules of rabbit polymorphonuclear leukocytes. *J. Cell Biol.* **66:**183–188.
18. FRYE, L. D., and M. EDIDIN. 1970. The rapid intermixing of cell surface antigens after formation of mouse heterokaryons. *J. Cell Sci.* **7:**319–336.
19. GOLDSTEIN, I. M., J. K. HORN, H. B. KAPLAN, and G. WEISSMAN. 1974. Calcium-induced lysozyme secretion from human polymorphonuclear leukocytes. *Biochem. Biophys. Res. Commun.* **60:**807–812.
20. GOODALL, R. J., and J. E. THOMPSON. 1971. A scanning electron microscope study of phagocytosis. *Exp. Cell. Res.* **64:**1–8.
21. HARTWIG, J. H., and T. P. STOSSEL. 1975. Isolation and properties of actin, myosin, and a new actin binding protein in rabbit alveolar macrophages. *J. Biol. Chem.* **250:**5696–5705.
22. HENSON, P. M. 1971. The immunologic release of constituents from neutrophil leukocytes. I. The role of antibody and complement on nonphagocytizable surfaces and phagocytosable particles. *J. Immunol.* **107:**1535–1546.
23. HIRSCH, J. G. 1956. Phagocytin: a bactericidal substance from polymorphonuclear leukocytes. *J. Exp. Med.* **103:**589–611.
24. HIRSCH, J. G. 1962. Cinemicrophotographic observations on granule lysis in polymorphonuclear leukocytes during phagocytosis. *J. Exp. Med.* **116:**827–834.
25. HIRSCH, J. G. 1974. Neutrophil leukocytes. *In*: The Inflammatory Process. Zweifach, B. W., Grant, L., and R. T. McClusky, editors. Academic Press, Inc., New York. **1:**411–447.
26. HITCHCOCK, S. E. 1977. Regulation of motility in nonmuscle cells. *J. Cell Biol.* **74:**1–15.
27. HORN, R. G., S. S. SPICER, and B. WETZEL. 1964. Phagocytosis of bacteria by heterophil leukocytes. Acid and alkaline phosphatase cytochemistry. *Am.*

J. Pathol. **45**:327–335.

28. KANE, R. E. 1975. Preparation and purification of polymerized actin from sea urchin extracts. *J. Cell Biol.* **66**:305–315.
29. KELLY, R. O., A. F. DEKKER, and J. E. BLUEMINK. 1973. Ligand-mediated osmium bindings: its application in coating biological specimens for scanning electron microscopy. *J. Cell Biol.* **59**(2, Pt. 2):165 *a* (Abstr.).
30. KORN, E. D., B. BOWERS, S. BATZRI, S. R. SIMMONS, and E. J. VICTORIA. 1974. Endocytosis and exocytosis: role of microfilaments and involvement of phospholipids in membrane fusion. *J. Supramol. Struct.* **2**:517–528.
31. LAWSON, D., M. C. RAFF, B. GOMPERTS, C. FEWTRELL, and N. B. GILULA. 1977. Molecular events during membrane fusion. A study of exocytosis in rat peritoneal mast cells. *J. Cell Biol.* **72**:242–259.
32. LEWIS, W. H. 1939. The role of a superficial plasmagel layer in changes in form, locomotion and division in tissue culture cells. *Arch. Exp. Zellforsch.* **23**:7–13.
33. LOCKWOOD, W. R., and F. ALLISON. 1963. Electronmicrographic studies of phagocytic cells. I. Morphological changes of the cytoplasm, and granules of rabbit granulocytes associated with ingestion of rough pneumococcus. *Brit. J. Exp. Pathol.* **54**:593–600.
34. LUFT, J. H. 1961. Improvements in epoxy resin embedding methods. *J. Biochem. Biophys. Cytol.* **9**:409–411.
35. MARUTA, H., and E. D. KORN. 1977. Purification from *Acanthamoeba castellani* of proteins that induce gelatin and syneresis of F-actin. *J. Biol. Chem.* **252**:399–402.
36. METCHINOFF, E. 1905. Immunity in Infectious Diseases (translated by F. G. Binnie). Cambridge University Press, London.
37. MOORE, P. L., H. BAND, and N. BRISSIE. 1975. The phagocytosis of bacteria by polymorphonuclear leukocytes: a freeze-fracture, SEM and thin section investigation. *J. Cell Biol.* **67**(2, Pt. 2):292 *a* (Abstr.).
38. MOORE, P. L., H. BANK, N. BRISSIE, and S. S. SPICER. 1976. Association of microfilament bundles with lysosomes in polymorphonuclear leukocytes. *J. Cell Biol.* **71**:659–666.
39. MOORE, P. L., J. S. CONDEELIS, D. L. TAYLOR, and R. D. ALLEN. 1973. Morphological identification of actin and myosin from *Chaos carolinensis*. *J. Cell Biol.* **59**(2, Pt. 2):232 *a* (Abstr.).
40. MOORE, P. L., P. L. SANNES, H. L. BANK, and S. S. SPICER. 1977. Membrane changes in polymorphonuclear leukocytes during ionophore-(A23187)-induced lysosomal release. Proceedings of the 35th Annual Meeting of the Electron Microscopy Society of America, Boston, Mass. 482–483.
41. MOOSEKER, M. S., and L. G. TILNEY. 1975. Organization of an actin-filament membrane complex. Filament polarity and membrane attachment in the microvilli of intestinal epithelial cells. *J. Cell Biol.* **67**:725–743.
42. NOSEWORTHY, J., G. H. SMITH, S. R. HIMMELHOCH, and W. H. EVANS. 1975. Protein and glycoprotein electrophoretic patterns of enriched primary and secondary granules from guinea pig polymorphonuclear leukocytes. *J. Cell Biol.* **65**:577–586.
43. OREN, R., A. E. FARNHAM, K. SAITO, E. MILOFSKY, and M. L. KARNOVSKY. 1963. Metabolic patterns in three types of phagocytising cells. *J. Cell Biol.* **17**:487–501.
44. PINTO DA SILVA, P. 1972. Translational mobility of membrane intercalated particles of human erythrocyte ghosts, pH-dependent reversible aggregation. *J. Cell Biol.* **53**:777–787.
45. PINTO DA SILVA, P., and D. BRANTON. 1970. Membrane splitting in freeze-etching. *J. Cell Biol.* **45**:598–605.
46. PINTO DA SILVA, P., S. D. DOUGLAS, and D. BRANTON. 1971. Localization of A antigen sites on human erythrocyte ghosts. *Nature (Lond.)*. **232**:194.
47. PINTO DA SILVA, P., and R. G. MILLER. 1975. Membrane particles on fracture faces of frozen myelin. *Proc. Natl. Acad. Sci. U. S. A.* **72**:4046–4050.
48. POLLARD, T. D., and E. D. KORN. 1973. Electron microscopic identification of actin associated with isolated amoeba plasma membranes. *J. Biol. Chem.* **248**:448–450.
49. POLLARD, T. D., and R. A. WEIHING. 1974. Actin and myosin and cell movement. *CRC Crit. Rev. Biochem.* **2**:1–65.
50. QUIE, P. G. 1972. Bactericidal function of human polymorphonuclear leukocytes. *Pediatrics.* **50**:264–270.
51. REYNOLDS, E. S. 1963. The use of lead citrate of high pH as an electron-opaque stain in electron microscopy. *J. Cell Biol.* **17**:208–212.
52. SATIR, B., C. SCHOOLEY, and P. SATIR. 1973. Membrane fusion in a model system: mucocyst secretion in *Tetrahymena*. *J. Cell Biol.* **56**:153–176.
53. SCHIFFMAN, E., B. A. CORCORAN, and S. M. WAHL. 1975. Formylmethionyl peptides as chemoattractants for leukocytes. *Proc. Natl. Acad. Sci. U. S. A.* **72**:1059–1062.
54. SCHOLLMEYER, J. V., D. E. GOLL, L. TILNEY, M. MOOSEKER, R. ROBSON, and M. STROMER. 1974. Localization of α-Actinin in nonmuscle material. *J. Cell Biol.* **63**(2, Pt. 2):304 *a*. (Abstr.).
55. SHEETZ, M. P., and S. J. SINGER. 1977. On the mechanism of ATP-induced shape changes in human erythrocyte membranes. I. The role of the spectrin complex. *J. Cell Biol.* **73**:638–646.
56. SHOWELL, H. J., R. J. FREER, S. H. ZIGMOND, E. SCHIFFMAN, A. S. WANIKUMAR, B. CORCORAN,

and E. L. BACKER. 1976. The structure-activity relations of synthetic peptides as chemotactic factors and inducers of lysosomal enzyme secretion for neutrophils. *J. Exp. Med.* **143:**1154–1169.

57. SINGER, S. J., and G. L. NICOLSON. 1972. The fluid mosaic model of the structure of cell membranes. *Science (Wash. D. C.).* **175:**720–731.
58. STECK, T. L. 1974. The organization of proteins in the human red blood cell membrane. A review. *J. Cell Biol.* **62:**1–19.
59. STEERE, R. L. 1969. Freeze-etching simplified. *Cryobiology* **5:**306.
60. STOSSEL, T. P., C. A. ALPER, and F. S. ROSEN. 1973. Serum-dependent phagocytosis of paraffin oil emulsified with bacterial lipopolysaccharide. *J. Exp. Med.* **137:**690–705.
61. STOSSEL, T. P., and J. H. HARTWIG. 1975. Interactions between actin, myosin, and an actin binding protein from rabbit alveolar macrophages. *J. Biol. Chem.* **250:**5706–5712.
62. STOSSEL, T. P., and T. D. POLLARD. 1973. Myosin in polymorphonuclear leukocytes. *J. Biochem.* **248:**8288–8294.
63. TAYLOR, D. L., J. S. CONDEELIS, P. L. MOORE, and R. D. ALLEN. 1973. The contractile basis of amoeboid movement. *J. Cell Biol.* **59:**378–394.
64. TILLACH, T. W., R. E. SCOTT, and V. T. MARCHESI. 1972. The structure of erythrocyte membranes studied by freeze-etching. *J. Exp. Med.* **135:**1209–1227.
65. TILNEY, L. G., and P. DETMERS. 1975. Actin in erythrocyte ghosts and its association with spectrin. *J. Cell Biol.* **66:**508–520.
66. TILNEY, L. G., and M. MOOSEKER. 1976. Actin filament-membrane attachment: are membrane particles involved? *J. Cell Biol.* **71:**402–416.
67. WEINSTEIN, R. S. 1969. Electron microscopy of surfaces of red cell membranes. *In*: Red Cell Membrane Structure and Function. G. A. Jamieson, and T. T. Greenwalt, editors. J. P. Lippincott Company, Philadelphia, Pa. 36.
68. WEINSTEIN, R. S., and N. SCOTT MCNUTT. 1970. Ultrastructure of red cell membranes. *Semin. Hematol.* **7:**259–274.
69. WETZEL, B., R. G. HORN, and S. S. SPICER. 1967. Fine structural studies on the development of heterophil, iosinophil, and basophil granulocytes in rabbits. *Lab. Invest.* **16:**349–382.
70. WETZEL, B. K. 1970. The fine structure and cytochemistry of developing granulocytes with special reference to the rabbit. *In*: Regulation of Hematopoiesis. A. S. Gordon, editor. Appleton-Century-Crofts, N.Y. **2:**769–817.
71. WHITE, J. G. 1973. The Chediak-Higashi syndrome. Fine structure of giant inclusions in freeze-fractured neutrophils. *Am. J. Pathol.* **72:**503–520.
72. WOOD, W. B., JR. 1953. Studies on the cellular immunology of acute bacterial infections. Harvey Lectures. Academic Press, Inc., New York. 72–98.
73. WRIGHT, D. G., and S. E. MALAWISTA. 1972. The mobilization and extracellular release of granular enzymes from human leukocytes during phagocytosis. *J. Cell Biol.* **53:**788–797.
74. VAN FURTH, R., and T. L. VAN ZWET. 1974. *In vitro* determination of phagocytosis and intracellular killing by polymorphonuclear and mononuclear phagocytes. *In*: Handbook of Experimental Immunology. D. M. Weir, editor. pg. 36.
75. ZUCKER-FRANKLIN, D., and J. G. HIRSCH. 1964. Electron microscopic study on the degranulation of rabbit peritoneal leukocyte during phagocytosis. *J. Exp. Med.* **120:**569–576.